Transactions of the Korean Nuclear Society Autumn Meeting
Gyeongju, Korea, October 26-27, 2017

Electron heat transport study in KSTAR using ECRH modulation

J.M. Ko, S.M. Yang, D.H. Na, Yong-Su Na* and KSTAR Team
Department of Nuclear engineering, Seoul National University, Seoul, Korea

**Corresponding author: ysna@snu.ac.kr*

1. Introduction

Exploring the energy transport in tokamak has been an important topic in fusion plasmas because the transport properties are closely linked with the fusion plasma confinement and the design of future tokamaks. Especially, the electron heat transport has been widely studied for a couple of decades. Previous researches showed that a part of profiles is insensitive to an auxiliary heating like ECRH (Electron Cyclotron Resonance Heating) [1-3]. Such a tendency to maintain the marginally stable profile is considered as a result of microturbulence because high value of the heat conductivity is beyond the neoclassical level [4,5].

There were numerous dedicated researches to figure out the electron heat conductivity χ_e using two classes of experimental method. The first class is the power balance [4,5,6] analysis of steady state plasmas. However, χ_e cannot be resolved by this static method alone so that the second class, the perturbative study, is adopted to provide complementary information [7]. Analyzing the amplitude and the phase can provide the information of the heat pulse propagation while applying a modulation of heat source.

However, perturbative analysis has been applied only to a local region at the early times. As an effort to establish a globally valid χ_e model, a simple model known as a CGM (Critical Gradient Model) was introduced which can be adopted in a wide range of the radius. CGM is a semi-empirically derived model and assumes that the electron heat flux and χ_e have a specific value of a threshold and a stiffness. The modulation experiments in JET [8,9], ASDEX [10,11], TCV [12] showed that their experimental results matched well with CGM. However, the perturbative analysis of the electron heat transport has not been studied in KSTAR before. In this work, recent electron heat source modulation experiments in KSTAR is described and the feasibility of CGM and its parameter dependencies in KSTAR are explored in L-mode plasmas.

2. Experimental Set Up and Methods

In these perturbative experiments, L-mode discharges were used in the KSTAR tokamak ($R = 1.8\,m$, $a = 0.5\,m$) with D2 plasmas. Four discharges (#18361, #18363 - #18365) with the high magnetic field B_T (2.2 T) and the low plasma current I_P (0.4 – 0.5 MA) were conducted to suppress the sawteeth effect. The electron density was set to prevent the distortion of the ECE (Electron Cyclotron Emission) signal by suprathermal electrons. During the ECRH modulation phases, the line averaged electron density $n_{e,l}$ was successfully feedback-controlled. Main plasma parameters in each discharge are described in Table I.

A 140 GHz ECRH was applied with 0.8 MW of heating power, changing resonance location in every shot from $\rho = 0.14$ to $\rho = 0.41$ in order to obtain low and high values of heat flux and the various electron temperature gradient R/LT_e (Fig. 1). During the current flat-top phase (1 – 10 s), the ECRH power was modulated at 3.5 – 7.5 s for the perturbative analysis while the steady ECRH phases were sustained in 2.5 – 3.5 s and 7.5 – 8.5 s of the discharges. The RF power deposition profile and the absorption rate is calculated by TORAY ray-tracing code in each shot.

The modulation frequency was set to be 20 Hz which showed the clearest signal than 10 and 30 Hz. The RF power was fully modulated. i.e., $maximum\ RF\ power - minimum\ RF\ power$ was 100%.

The plasma current density and the safety factor q profiles were reconstructed by using the EFIT equilibrium code. The measurement of the electron temperature T_e is provided by the ECE diagnostic with the $0.01\,ms$ resolution, and the ion temperature was measured by the CES diagnostics. Neutral beam injection (NBI) blips were applied at every second in the flat-top phase for the CES measurement. $n_{e,l}$ was measured by the interferometer and the electron density n_e profiles were obtained by the Thomson scattering diagnostics.

Table I: Main plasma parameters

	18361	18363	18364	18365
B_T (T)	2.2	2.2	2.2	2.4
I_P (MA)	0.5	0.4	0.4	0.4
ECH Location	$\rho = 0.38$	$\rho = 0.4$	$\rho = 0.4$	$\rho = 0.14$
ECH Power (MW)	0.8	0.8	0.8	0.8
$T_{e,0}$ (keV)	2.2	1.5	1.5	4
$n_{e,l}$ (m^{-3})	1.9	2.4	2.5	2.4
Z_{eff}	2.0	2.0	2.0	2.0
q_0	1.3	1.7	1.7	1.3
q_{95}	5.5	7	7	7.5

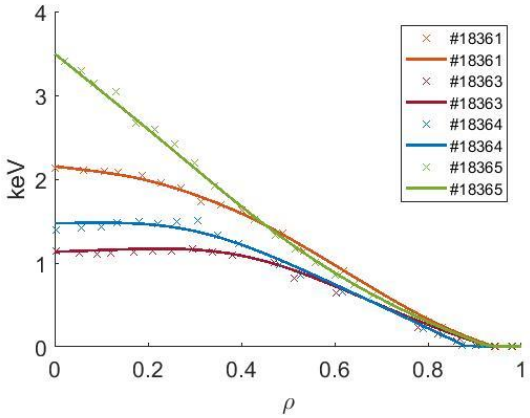

Fig. 1. The electron temperature profiles in normalized radius for various ECRH deposition profiles.

3. Analysis Method

In this section, the static analysis and the dynamic analysis will be described in 3.1 and 3.2 respectively. The transport models used in each method will also be described.

3.1 Power Balance Analysis

In steady-state, we can obtain the electron heat conductivity χ_e by the power balance method which consider the input power and the output power. In this work, input power is ohmic power and RF power, and the output power is from exchange power of electron-ion, radiation, and the collision with neutrals. Ignoring the convective term, the experimental χ_e obtained from the power balance analysis is

$$\chi_e = -\frac{q_e}{n_e \nabla T_e} \quad (1)$$

In our experiments, two steady ECRH phases in flat-top were used for power balance analysis in #18363-#18365, and one steady phase in #18361 that has only one steady phase in flat-top.

3.2 Perturbative Analysis

In experiments, a modulation of the heating source can show how the perturbation propagates in plasmas while keeping other variables almost constant. If we analyze the amplitude and the phase obtained from the Fourier transform, we can discover the information of the propagation which can only be seen in the frequency domain. For example, the phase is minimum and the amplitude is maximum where the ECRH is injected. Similarly, plasma parameters affect the shape of the amplitude and the phase profiles. In case of our study, these information makes the number of solutions reduced that are not unique with the power balance analysis alone.

For perturbative analysis, time evolutions of T_e are FFT transformed at each radial point. Phase reference was set to the phase of the RF power. In each shot, LFS (Low Field Side) T_e profiles were chosen for the FFT analysis.

4. Turbulent Transport Model

The critical gradient model expressed in [13] is expressed as

$$\chi_e = \chi_{GB}[\,\chi_s \left(\frac{R}{LT_e} - \kappa\right) H\left(\frac{R}{LT_e} - \kappa\right) + \chi_0] \quad (2)$$

Here, q is the safety factor, H(x) is a Heaviside function, and χ_e is normalized by the Gyro-Bohm scale $\chi_{GB} = q^{\nu} \frac{T}{eB} \frac{\rho_s}{R}$. χ_0, χ_s, and κ_c are free-parameters which characterizes the residual flux, the stiffness, and the threshold, respectively. In this paper, these parameters are assumed to be constant in all region for simplicity. These parameters can affect not only T_e but also the harmonics of amplitudes and phases.

Although there were no obvious value of ν in this model, ν is known to have a range of 1-2. In our case, ν is selected as 1.5 which shows the best fit in KSTAR as in other devices [13,14].

5. Results

Three parameters, χ_0, χ_s, and κ_c are adjusted to best reproduce the KSTAR experimental results. Referring to the previous studies in other devices [13], the ranges of χ_s, χ_0, κ were set to 0.01-3.01, 0.01-3.01, and 2-8, respectively. The values of three parameters were scanned with the interval of 0.05, 0.05, and 1 to figure out which value minimizes both the amplitude error and the phase error. Considering the turbulent regime, the errors were calculated as the average of the variation from the experimental values in the region of $\rho = 0.3 - 0.7$. For example, χ_s is chosen to be 0.29 instead of 0.09 and 0.49 in #18364 discharge as shown in Fig. 2. The point is, even though $\chi_0 = 0.23$ is closer with the experimental profiles in the amplitude, $\chi_0 = 0.43$ is selected because the phase error with $\chi_0 = 0.23$ is much larger than that with $\chi_0 = 0.43$.

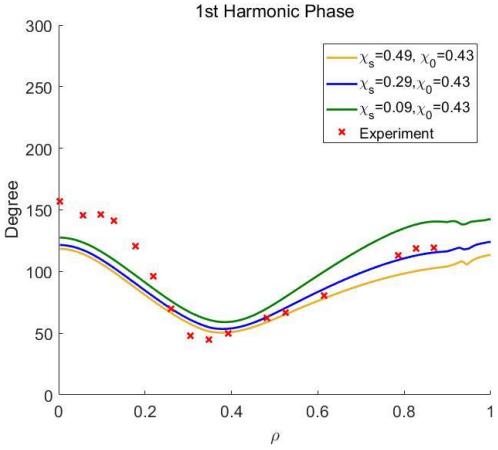

Fig. 2. The 1st harmonic phase profile in normalized radius of #18364 (Off-axis). $\chi_s = 0.43$, $\chi_0 = 0.29$ (blue line) exhibits the best fit to the experiment (red cross).

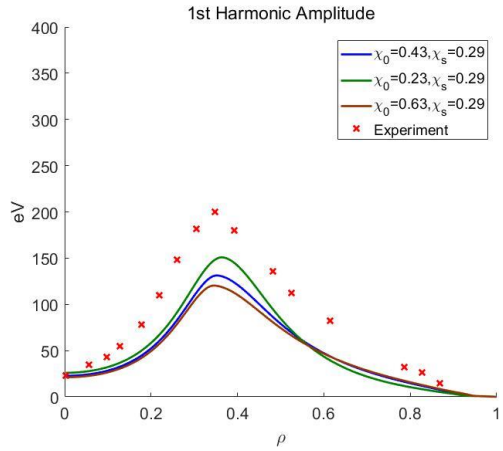

Fig. 2. The 1st harmonic amplitude profile in normalized radius of #18364 (Off-axis). $\chi_s = 0.43$, $\chi_0 = 0.29$ (blue line) shows the best fit to the experiment (red cross). $\chi_s = 0.23$, $\chi_0 = 0.29$ (green line) is not selected due to the bigger phase difference.

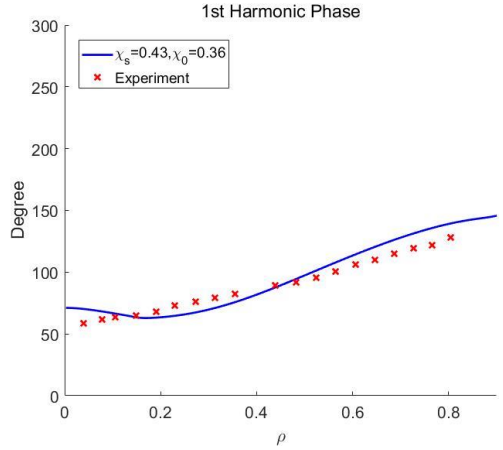

Fig. 3. The 1st harmonic phase profile in normalized radius of #18365 (On-axis). $\chi_s = 0.43$, $\chi_0 = 0.36$ (blue line) exhibits the best match to experiment (red cross).

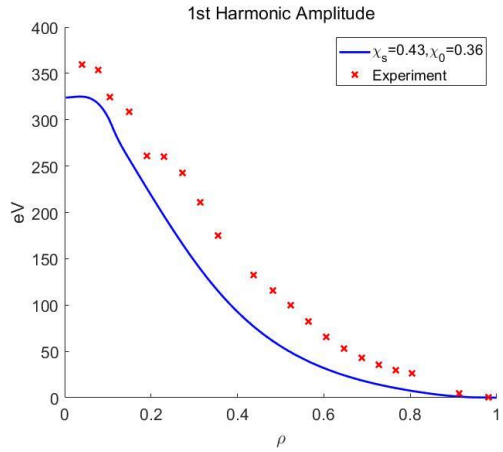

Fig. 4. The 1st harmonic amplitude profile in normalized radius of #18365 (On-axis). $\chi_s = 0.43$, $\chi_0 = 0.36$ (blue line) reproduces the experiment the best (red cross).

According to the above criterion, proper values of χ_0, χ_s, and κ_c were determined in the four discharges.

Table II: Free-Parameters in the critical gradient model

	χ_s	χ_0	κ
18361	0.51	0.31	4
18363	0.36	0.41	4
18364	0.29	0.43	3
18365	0.43	0.36	7

With the determined free-parameters shown in Table II, the electron heat flux with CGM is compared with the power balance results as presented in Fig. 5-7. Heat fluxes are normalized to the gyro-Bohm scale, $q_{e,GB} = q_e/(q^{1.5}n_eT_e^2\rho_s/eBR^2)$ [9]. The CGM model in the on-axis heating shot (red line) considerably differs from other shots in $\rho = 0.4$ and $\rho = 0.5$. As ρ goes to $\rho = 0.6$, the gradient of T_e in the on-axis heating shot gets similar with other shots so that the gap from other lines decreases. Most importantly, the CGM model obtained from the perturbative analysis is well-matched with the results from the power balance result.

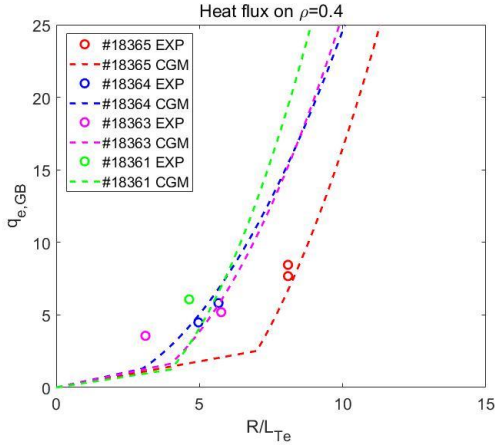

Fig. 5. Gyro-Bohm scale normalized electron heat flux at $\rho = 0.4$ Dashed lines are the critical gradient model found in the perturbative analysis (Table II). Circles are the experimental χ_e which obtained from the power balance analysis.

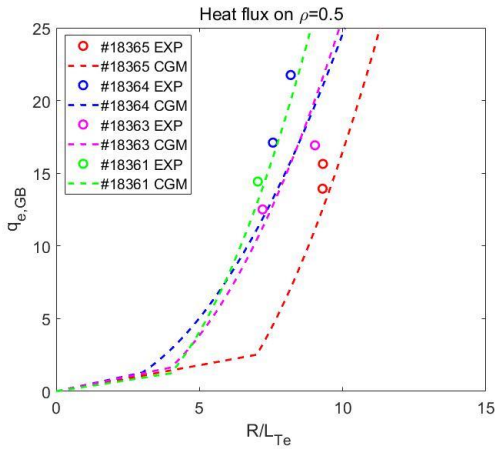

Fig. 6. Gyro-Bohm scale normalized electron heat flux at $\rho = 0.5$ Dashed lines are the critical gradient model found in the perturbative analysis (Table II). Circles are the experimental χ_e which obtained from the power balance analysis.

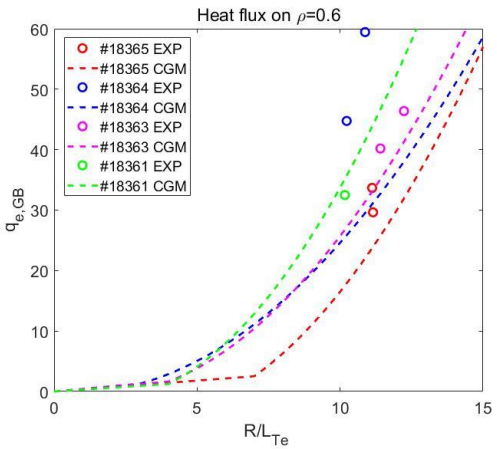

Fig. 7. Gyro-Bohm scale normalized electron heat flux at $\rho = 0.6$ Dashed lines are the critical gradient model found in the perturbative analysis (Table II). Circles are the experimental χ_e which obtained from the power balance analysis.

In terms of χ_s and χ_0, the values seem to exist in a range of χ_s and χ_0 obtained in other devices [13] though it is difficult to find clear dependencies on plasma parameters. On the other hand, the threshold κ seems to have a dependency with the magnetic shear which is a major difference between #18365 and other shots.

6. Conclusion

ECRH modulation experiments and perturbative analysis were conducted in KSTAR L-mode plasmas using the semi-empirical model, CGM. We can obtain a simple model and determine the free-parameters by using the amplitude and phase information in the experiment.

Small differences are found between the experimental values and simulated results. The discrepancy in the core may be due to the neoclassical collision which is known to be more dominant than turbulent fluxes in that region. In addition, the difference in the shape of phases and amplitudes is probably a result from the radial dependencies of free-parameters which we assumed to be constant in this work. Applying a weighting or a parameter dependency might improve the model more realistically.

Despite a small discrepancy in some regions, CGM reproduces the electron conductivity quite well in a turbulent dominant region. Especially, the experiment shows a possibility of the plasma parameter dependence of the electron heat conductivity χ_e in KSTAR. If more experimental data is accumulated, further study can provide a clue for predicting the turbulent properties of the electron transport in KSTAR by using a simple model.

REFERENCES

[1] R. Goldston, et al, Proc. 11th Int. Conf. on Plasma Physics and Controlled Nuclear Fusion Research (Kyoto,1986), Vol. 1 (Vienna: IAEA), pp 75, 1987.

[2] F. Wagner, et al, “Experimental study of the principles governing tokamak transport.", Physical review letters, Vol. 56, No. 20, 1986.

[3] T. C. Luce, C. C. Petty, and J. C. M. De Haas. "Inward energy transport in tokamak plasmas.", Physical review letters, Vol. 68, No. 1, 1992.

[4] F. Ryter, et al, "Experimental characterization of the electron heat transport in low-density ASDEX upgrade plasmas.", Physical review letters, Vol. 86, No. 24, pp. 5498 – pp. 5501, 2001.

[5] G. T. Hoang, et al, "Experimental determination of critical threshold in electron transport on Tore Supra.", Physical review letters, Vol. 87, No. 12, 125001, 2001.

[6] G. T. Hoang, et al, "Magnetic shear effects on confinement and electron heat transport in Tore Supra discharges with electron heating.", Nuclear Fusion, vol. 38, No. 1, pp. 117-132, 1998.

[7] NJ Lopes. Cardozo, "Perturbative transport studies in fusion plasmas.", Plasma physics and controlled fusion, Vol. 37, No. 8, pp. 799.-852, 1995.

[8] P. Mantica, et al, "Transient heat transport studies in JET conventional and advanced tokamak plasmas.", Proc. 19th Int. Conf. on Fusion Energy, 2002.

[9] N. Bonanomi, et al, "Trapped electron mode driven electron heat transport in JET: experimental investigation and gyro-kinetic theory validation.", Nuclear Fusion, Vol. 55, No. 11, 113016, 2015.

[10] F. Imbeaux, F. Ryter, and X. Garbet, "Modelling of ECH modulation experiments in ASDEX Upgrade with an empirical critical temperature gradient length transport model.", Plasma physics and controlled fusion, Vol. 43, No. 11, 1503, 2001.

[11] F. Ryter, et al, "Electron heat transport in ASDEX Upgrade: experiment and modelling.", Nuclear fusion, Vol. 43, No. 11, 1396, 2003.

[12] Y. Camenen, et al, "Electron heat transport studies under intense EC heating in TCV.", IAEA Technical Meeting on ECRH Physics and Technology for ITER (F1-TM-26015), Kloster Seeon, Germany, 2003.

[13] X. Garbet, et al, "Physics of transport in tokamaks.", Plasma Physics and Controlled Fusion, Vol. 46, No. 12, pp. B.557-B574, 2004.

[14] X. Garbet, et al, "Profile stiffness and global confinement.", Plasma physics and controlled fusion, Vol. 46, No. 9, pp. 1351-1373, 2004.